A minicourse on

SOLAR ROTATION

K. Petrovay
Eötvös University, Department of Astronomy
Budapest, Hungary
K.Petrovay@astro.elte.hu

HISTORY

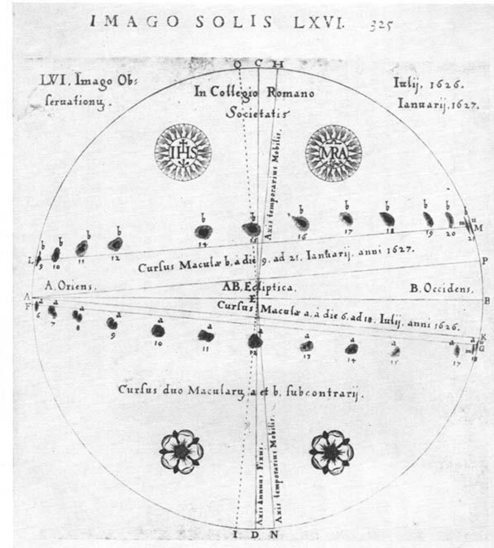

1610: First telescopic observations
of sunspots. Sun rotates.

1858: R. Carrington, MNRAS 19, 1: exact determination of rotation rate ("Carrington rate"),
based on a well planned series of observations (1853-61).
Sidereal rate: $\overline{\Omega}_C = 14°11'/\mathrm{day}$; Mean synodic rate: $13°12'/\mathrm{day}$
Sidereal period $\overline{P}_C = 25^{\mathrm{d}}\!.38$; synodic period $27^{\mathrm{d}}\!.2753$).
"Rotation no. 1" started on 9 Nov 1853.
Rotational elements: $i_C = 7.25°$, $\hat{\Omega}_C = 73.67°$. (Actually, $i = 7.12°$ — Balthasar et al. 1987)

1863: Carrington: *Observations of the Spots on the Sun.* London
Differential rotation discovered and described as $\Omega = A + B \sin^{7/4}\Phi$.

1906: Duner detects solar rotation from Doppler shift of spectral lines at 2 points on solar disk.

1960's: Doppler compensator

1989: Helioseismic determination of internal rotation

METHODS

– Plasma rotation
  - Doppler
  - Helioseismology (eigenmodes split according to azimuthal order m)
– Tracers
  - Individual tracers (short-term/small-scale correlation tracking)
    - Sunspots
    - Faculae
    - Magnetic elements
    - Filaments
    - ...
  - Patterns (long-term/large-scale correlation tracking)
    - Unipolar areas in photosphere
    - Coronal holes
    - Interplanetary sector boundaries
    - ...

DESCRIPTION OF DIFFERENTIAL ROTATION

$\Omega = f(\Phi)$. Expand on an orthogonal basis, e.g. Legendre polynomials:

$$\Omega = \sum_i C_i P_{2i}(\sin\Phi) \qquad (\text{ N.B. } \sin\Phi = \cos\theta)$$

$$P_0(\sin\Phi) = 1 \qquad P_2(\sin\Phi) = \tfrac{1}{2}(3\sin^2\Phi - 1) \qquad P_4(\sin\Phi) = \tfrac{1}{8}(35\sin^4\Phi - 30\sin^2\Phi + 3)$$

$$\Rightarrow \boxed{\Omega = A + B\sin^2\Phi + C\sin^4\Phi} \qquad \text{where}$$

$$A = C_0 - \tfrac{1}{2}C_2 + \tfrac{3}{8}C_4 \qquad B = \tfrac{3}{2}C_2 - \tfrac{30}{8}C_4 \qquad C = \tfrac{35}{8}C_4$$

Attention:

1, $\sin^2$ and $\sin^4$ are not orthogonal

$\Rightarrow$ **errors in A, B and C are not independent**, unlike in C_i's.

Actually, a better choice are Gegenbauer polynomials, orthogonal on a disk, rather than a sphere - cf. Snodgrass 1984).

$\sin^4\Phi$ only important at high latitudes $\Rightarrow$ usually neglected for sunspots.

Things to care about: sidereal or synodic? Ω or $\Omega/2\pi$?

Dimensions of coefficients: 1μrad/s $= 1/2\pi\,\mu$Hz $= 86400 \cdot 10^{-6} \cdot 360/2\pi°$/day$= 4.95°$/day

PLASMA ROTATION

Doppler measurements by Doppler compensator from the 1960s onwards. Precision 15–40 m/s.

Classic determination: Howard & Harvey (1970, SPh 12, 23), from Mt.Wilson magnetograms, for 1966-68:

$$A = 2.78 \pm 0.003 \qquad B = -0.351 \pm 0.03 \qquad C = -0.443 \pm 0.05 \qquad \text{Mean rate: } \overline{\Omega} = 13.76^\circ/\text{day}$$

Snodgrass: $A = 452\,\text{nHz}$; $\quad B = -49\,\text{nHz}$; $\quad C = -84\,\text{nHz}$

Many other determinations.

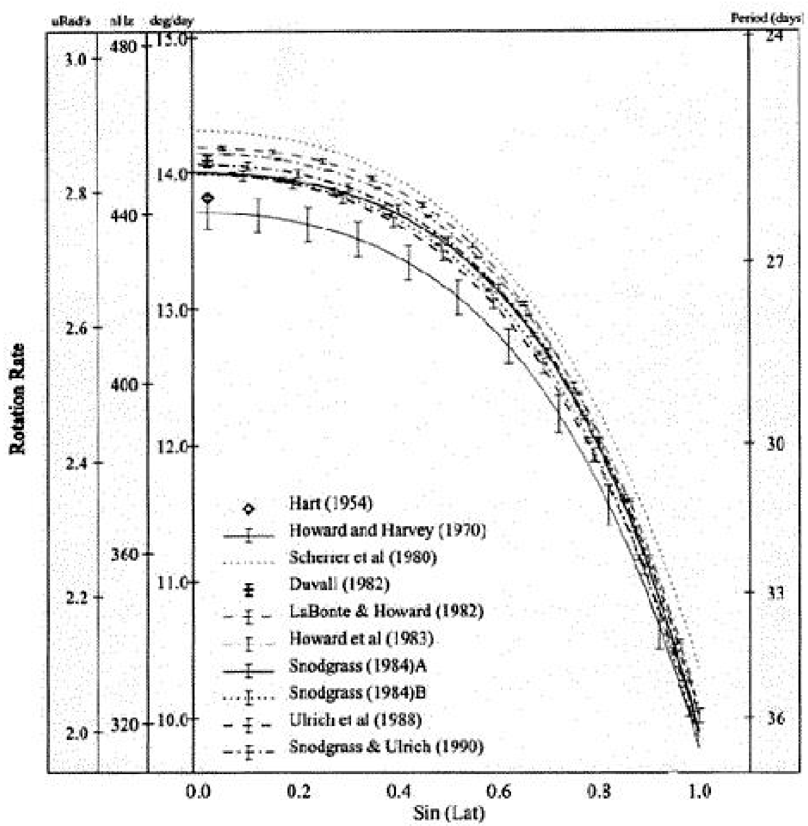

Seismic determination of plasma rotation

First splitting data: Brown (1985)

First good inversions:

- Brown, Christensen-Dalsgaard, Dziembowski, Goode, Gough & Morrow (1989);
- Dziembowski, Goode & Libbrecht (1989): $A = 455.4\,\mathrm{nHz}$; $B = -52.4\,\mathrm{nHz}$; $C = -84.1\,\mathrm{nHz}$

GONG results: Thompson et al. (1996, Science 272, 1300)

MDI results: Schou et al. (1998)

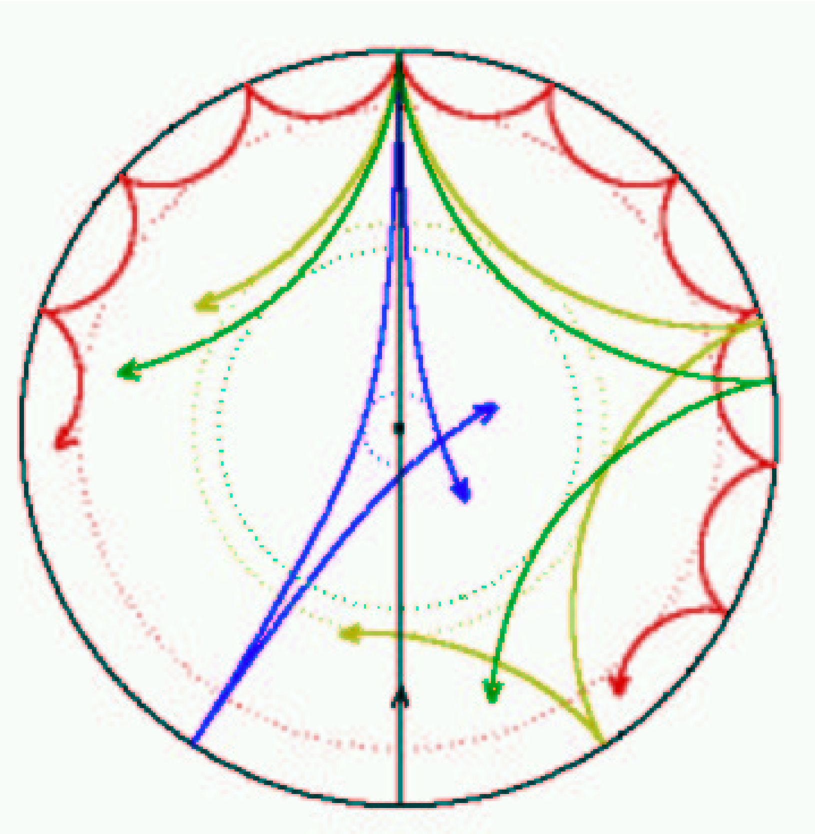

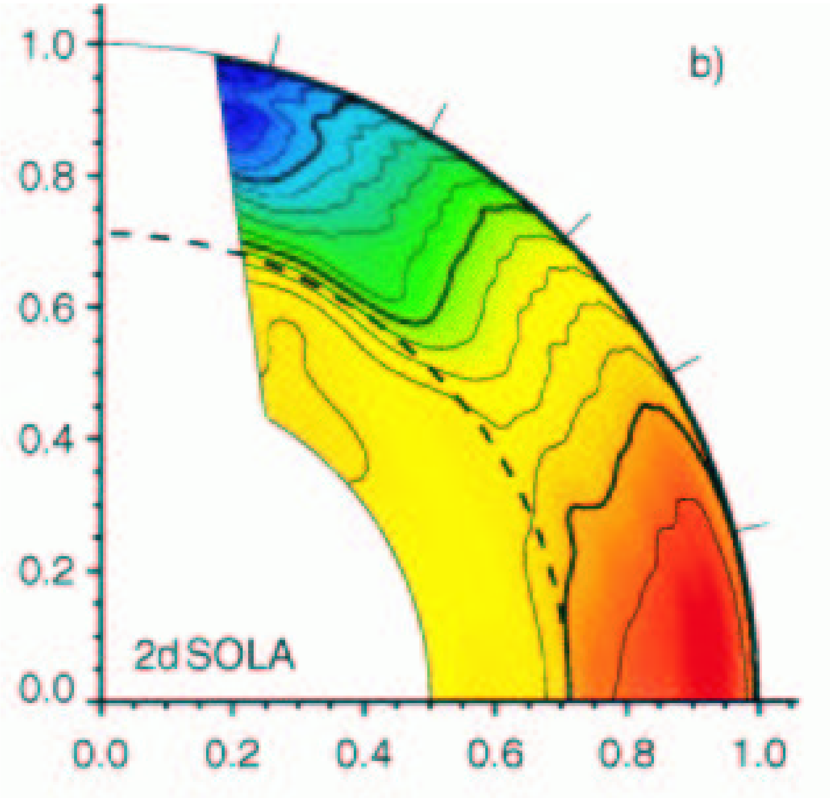

ORIGIN OF DIFFERENTIAL ROTATION

Observation:

Diff.rotation similar in Sun and giant planets. What's common to them?

They are *fast rotators:* Coriolis number $\mathrm{Co} = \tau\Omega \gg 1$. ($\tau$: (Eulerian) correlation time of turbulence.)

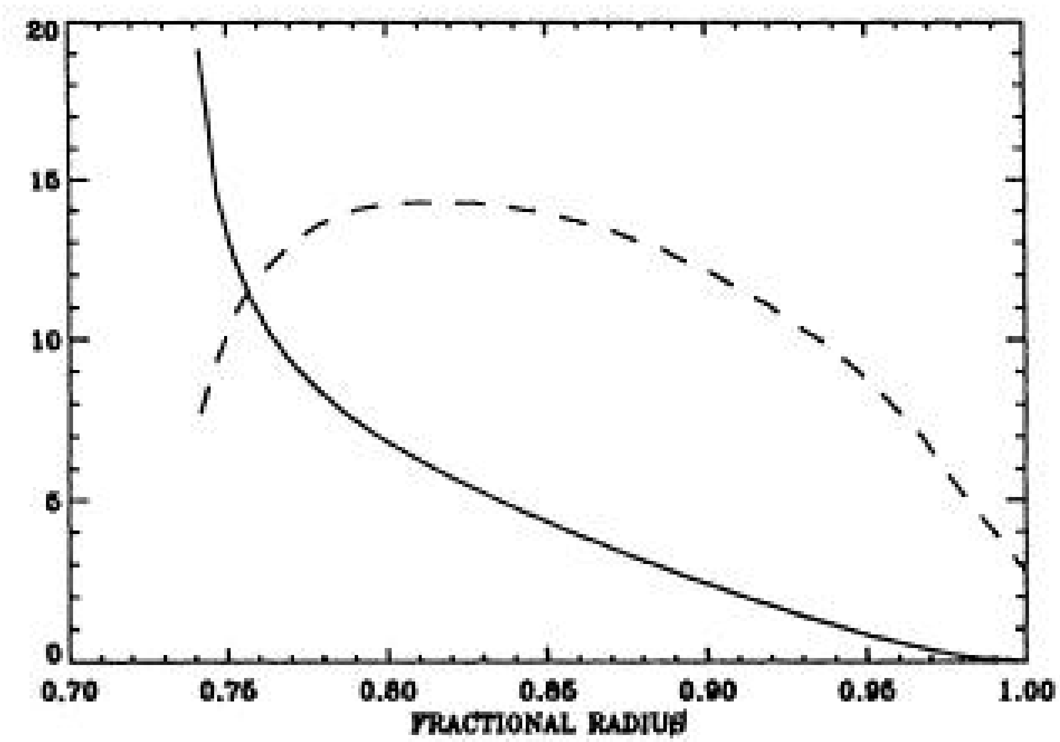

Fig. 1. The dependences of the Coriolis number, $\Omega^* = 2\tau_{corr}\Omega$ (full line), and the normalised viscosity, $\nu_T/(10^{12}\,cm^2 s^{-1})$ (broken), on fractional radius, $x = r/R$, for the Stix model of the convection zone

Origin of differential rotation, schematically

Rotation + turbulent convection

In rigid rotator $\Rightarrow \overline{v_\theta v_\phi} = \Lambda_V \cos\theta\,\Omega > 0$. ("$\Lambda$ effect"): angular momentum transfer towards equator

$\Rightarrow$ pole–equator difference increases until turbulent viscosity allows, i.e. $\overline{v_\theta v_\phi} = \Lambda_H \cos\theta\,\Omega - \nu_T \dfrac{\partial\Omega}{\partial\theta} = 0$

Essence of Λ-effect:

Coriolis force deflects to right on N hemisphere

$\Rightarrow$ turb. fluid parcels rotating faster go towards equator

fluid parcels rotating slower go towards pole

$\Rightarrow$ equatorial acceleration, polar deceleration

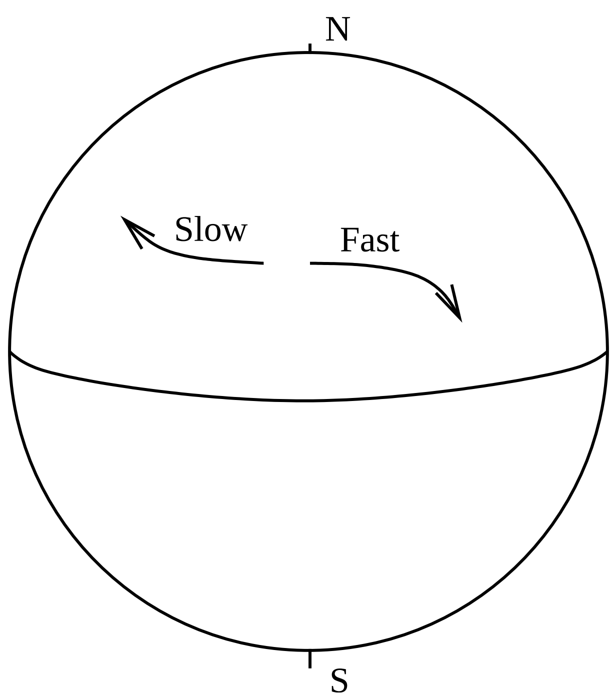

Details:

Turb. element of speed v_ϕ.
Horizontal Coriolis acceleration is $2\Omega v_\phi \cos\theta$.

In the parcel's lifetime (Lagrangian corr.time) τ_L
this imparts to it a velocity $v_\theta = 2\mathrm{Co}_L\, v_\phi \cos\theta$

$\Rightarrow 2\mathrm{Co}_L\, \overline{v_\phi^2} \cos\theta$ contribution to $\overline{v_\theta v_\phi}$.
$(\mathrm{Co}_L \simeq \mathrm{Min}\,[\mathrm{Co}\,,1])$

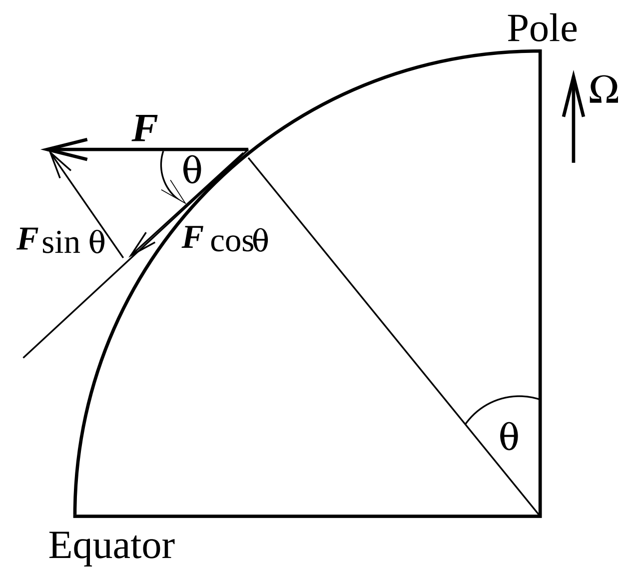

Parcels moving in a meridional direction contribute with the opposite sign; the two together yield:

$\boxed{\overline{v_\theta v_\phi} = 2\mathrm{Co}_L\, (\overline{v_\phi^2} - \overline{v_\theta^2}) \cos\theta}$ Similarly: $\boxed{\overline{v_r v_\phi} = 2\mathrm{Co}_L\, (\overline{v_\phi^2} - \overline{v_r^2}) \sin\theta}$

Slow rotation (Co $\ll 1$): $\overline{v_r^2} > \overline{v_\phi^2} \simeq \overline{v_\theta^2}$ $\Rightarrow$ no latitudinal diff.rot.; radial subrotation (outer layers slower)

(Note.: In Kitchatinov's quasiisotropic theory radial superrotation —incorrect.)

But: for thin ($\ll H_P$) conv.zone $\overline{v_r^2} < \overline{v_\phi^2} \simeq \overline{v_\theta^2} \Rightarrow$ no latitudinal diff.rot.; radial superrotation

Fast rotation (Co $\gtrsim 1$):

Case (1): Convective rolls

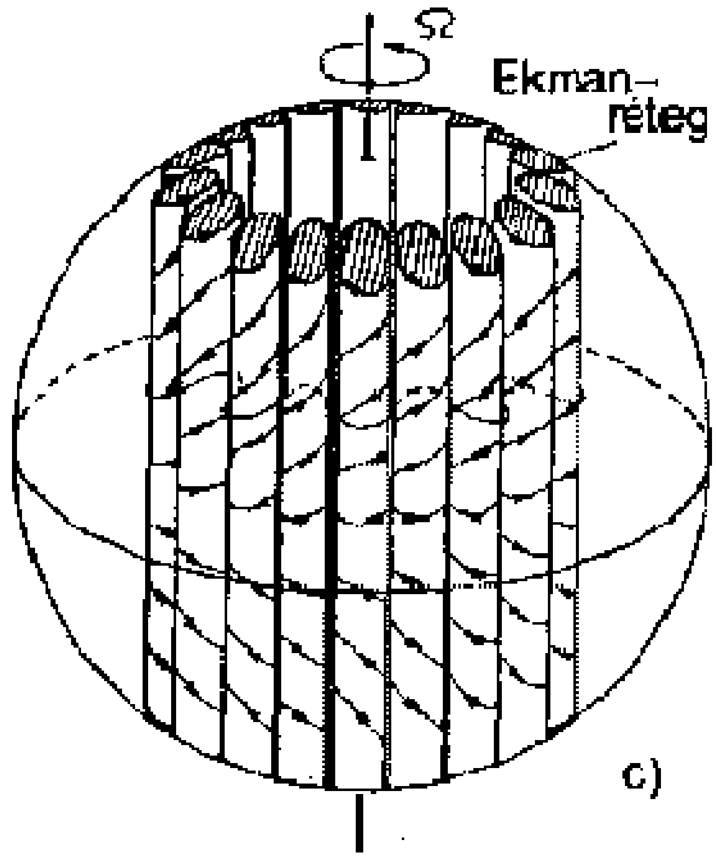

$\overline{v_\phi^2} \sim \overline{v_r^2}/\sin^2\theta \sim \overline{v_\theta^2}/\cos^2\theta \Rightarrow$ Disk-like isorotational surfaces

$\Rightarrow$ Equatorial acceleration; radial diff.rot. weak on equator; significant subrotation near poles

Case (2): Banana cells

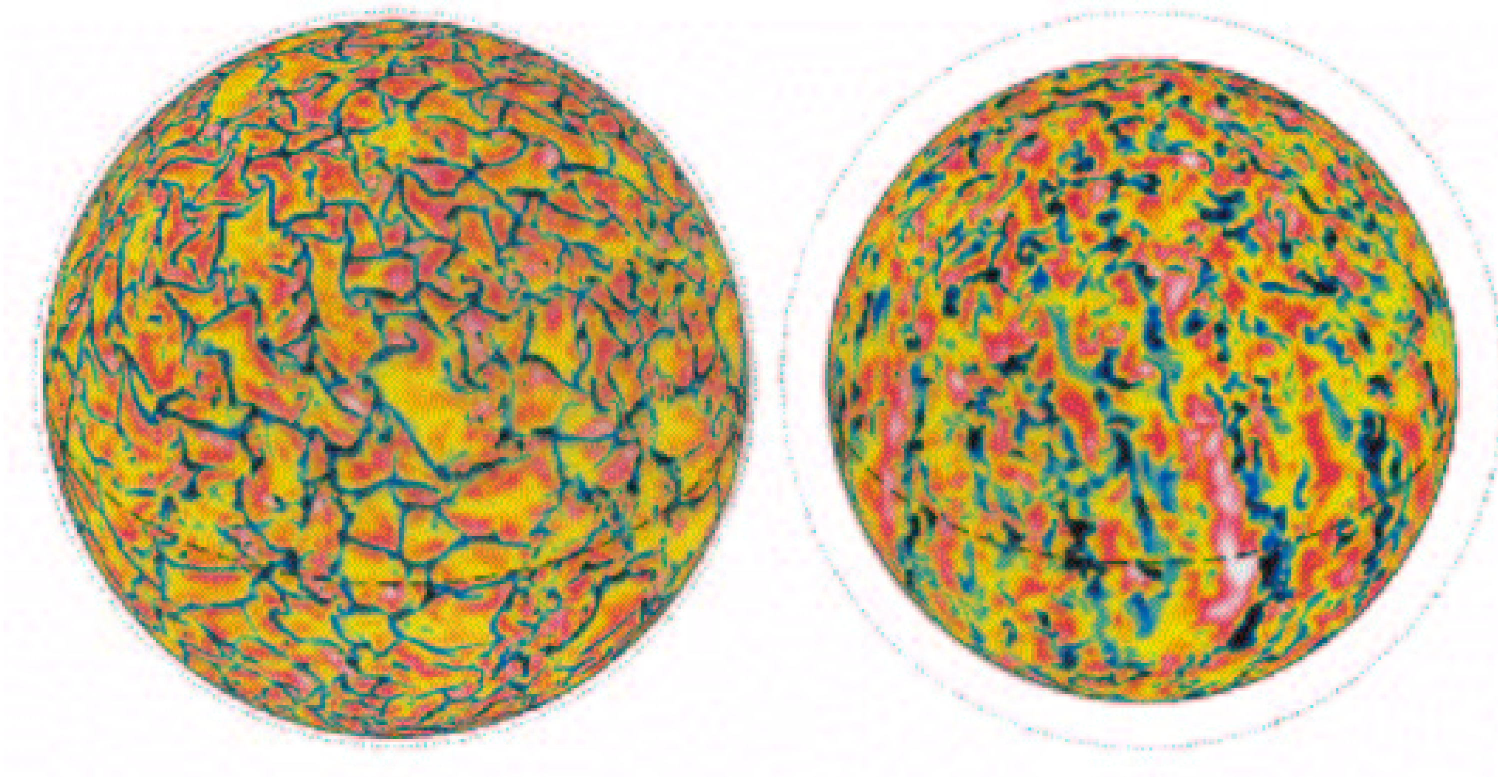

(Brun & Toomre 2002)

$\overline{v_\phi^2} \simeq \overline{v_r^2} > \overline{v_\theta^2}/\cos^2\theta \Rightarrow$ Cone-like isorotational surfaces

$\Rightarrow$ Equatorial acceleration; no radial diff.rot.

n Sun we expect: Banana cells in bulk of CZ;
+ subrotation near surface (where Co < 1).

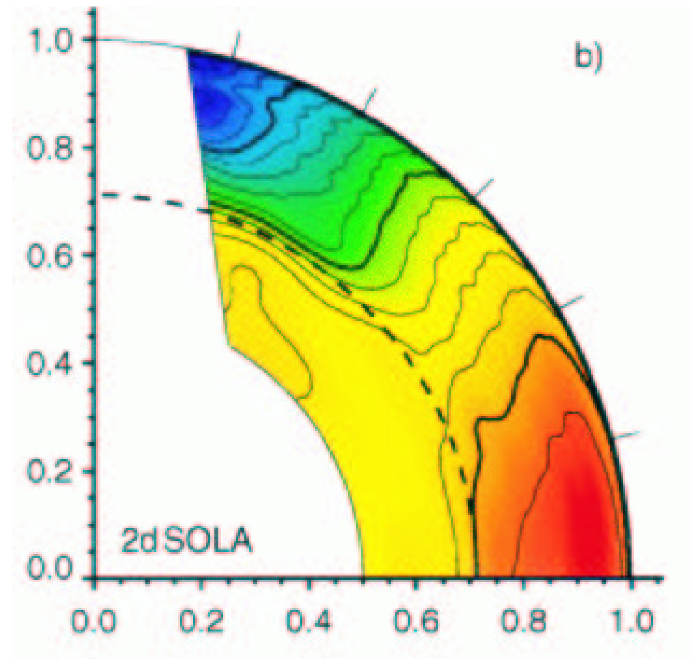

n some stars diff.rot. is apparently inverse. How could this come about?

Effect of meridional circulation:

Drives system towards $\Omega \propto a^{-2}$ (constant specific angular momentum) $\Rightarrow$ if very strong, pole may even be aster.

Effect of magnetic field:

Strong toroidal field $\Rightarrow \overline{v_\theta^2} \sim \overline{v_r^2} \gg \overline{v_\phi^2} \Rightarrow$ Equatorial deceleration, radial subrotation

Tidal effects in close binaries:

– Tidal locking; most effective on equator.

– If equator $\neq$ orbital plane, tides may lead to strong meridional motions $\Rightarrow$ faster pole?

Detailed modelling of differential rotation

Mean field approach

Nondiffusive fluxes written as

$$\overline{v_\theta v_\phi} = \Lambda_H \cos\theta\, \Omega$$

$$\overline{v_r v_\phi} = \Lambda_V \sin\theta\, \Omega$$

Fourier expansion of Λ in θ, with considerations of symmetry and continuity

$$\Lambda_V = \nu_T \left[V^{(0)}(r) + V^{(1)}(r) \sin^2\theta + \ldots \right]$$

$$\Lambda_H = \nu_T \left[H^{(1)}(r) \sin^2\theta + \ldots \right].$$

Coefficients evaluated from effect of rotation on isotropic turbulence.

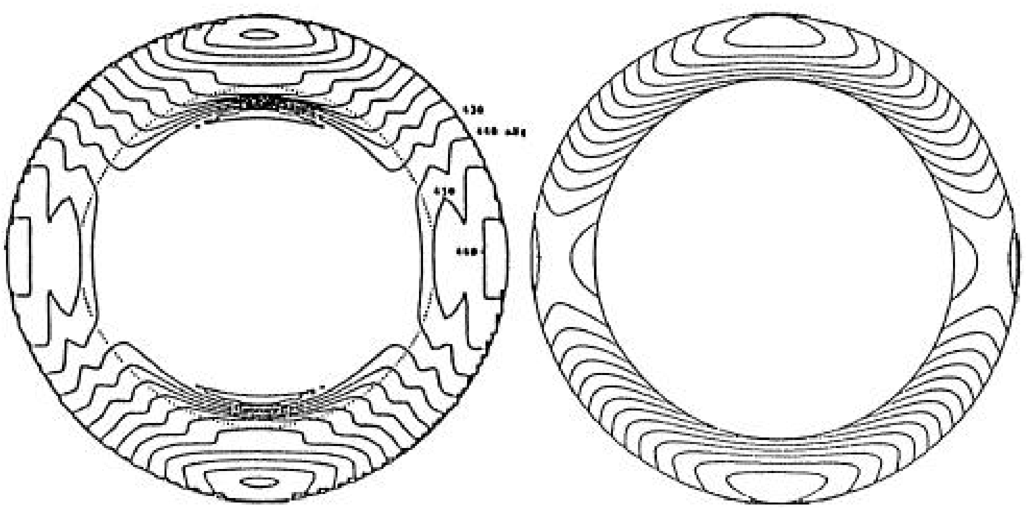

Fig. 3. Angular velocity isolines from helioseismology (Libbrecht 1988; left) and our model (right). The contour levels in both sides of the figure are the same

(Küker et al. 1993)

Parameter calibration by local simulations

Parameters of mean field models can be calibrated from simulations of rotating convection. E.g. Rüdiger & Chan (2001): f-plane simulations for subsurface layers yield

l	$V^{(l)}$	$H^{(l)}$
0	−0.300	N/A
1	0.187	0
2	0.0158	0
3	0.0337	0.727

This corrects incorrect superrotation near surface in pure mean field models.

Global simulations

From 1980's (Glatzmaier 1989).

Latest version: Brun & Toomre (2002); Miesch (2002).

Still tends to lead to cylindrical isorotation surfaces, though keeps improving.

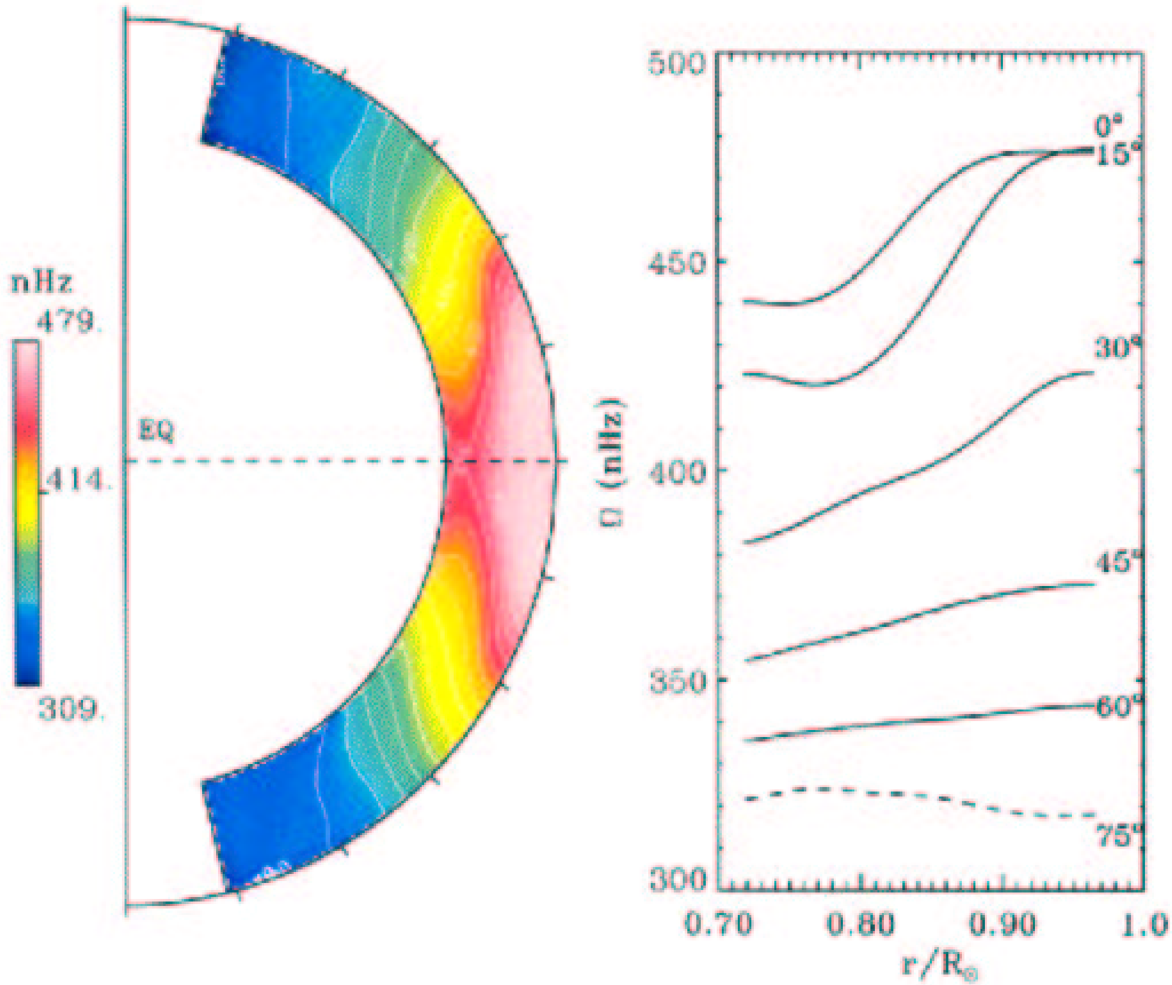

(Brun & Toomre 2002)

TRACER ROTATION

Generally slightly faster than plasma near equator, and slightly stronger diff.rot.

Classic measurement:

Newton & Nunn (1951) for recurrent spots:

$A = 14\overset{\circ}{.}38/\text{day} \qquad B = -2\overset{\circ}{.}77/\text{day}$

Young spots rotate faster, and are decelerating.

Snodgrass (1983) mg. features: A=462 nHz; B=-74 nHz C=-53 nHz

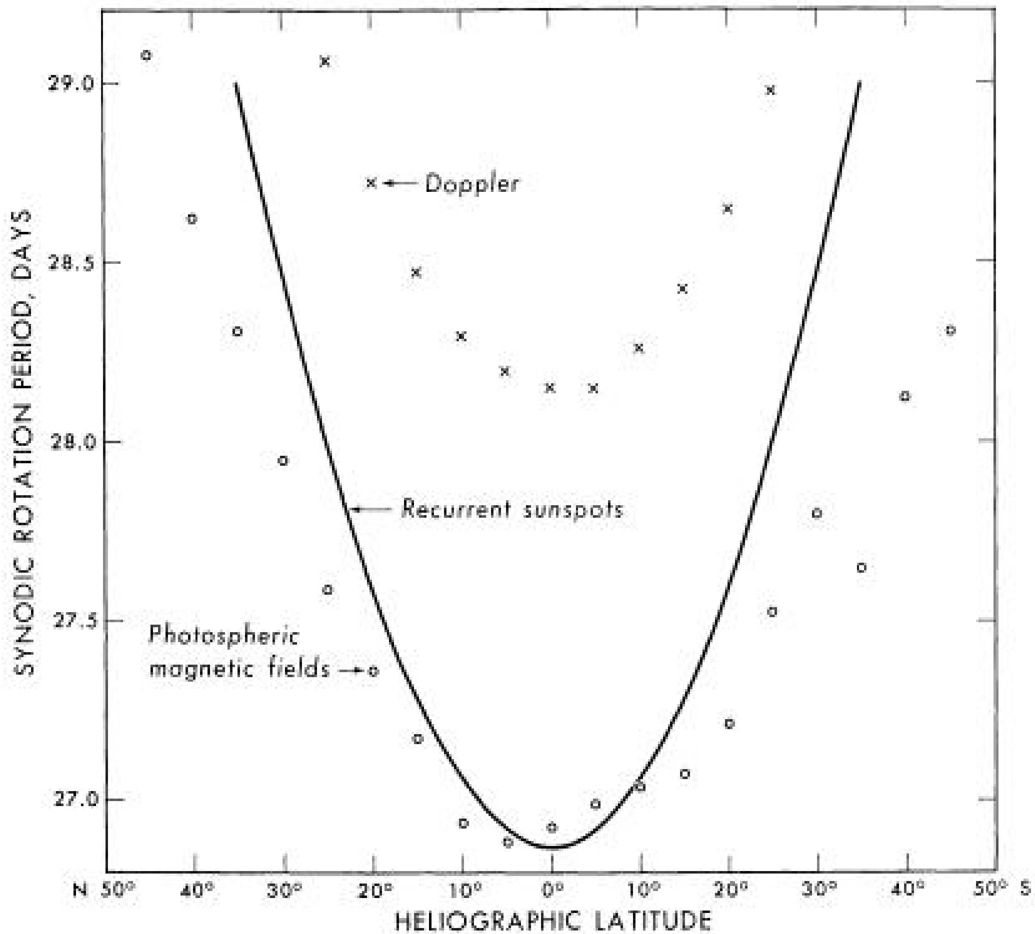

nterpretations:

(a) Corks.

Clearly wrong

(b) Anchoring.

Naive.

(c) Magnetic tree.

Projection effects, wavelike phenomena, artifacts.

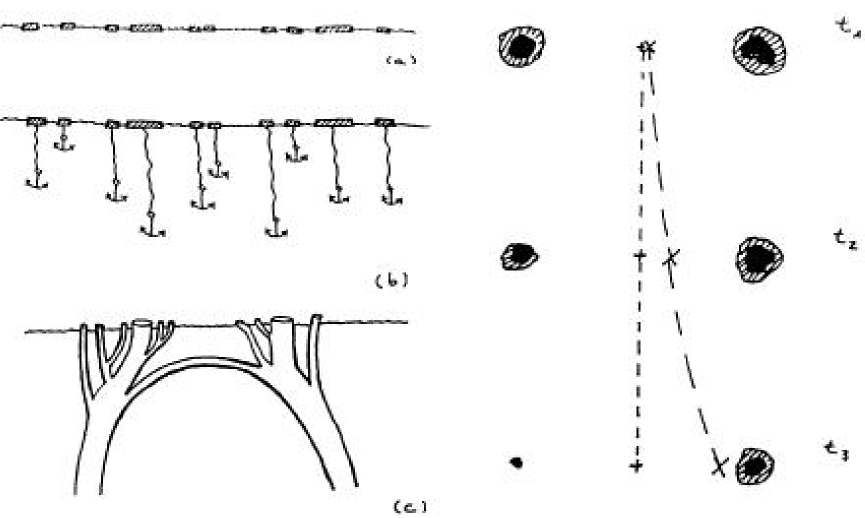

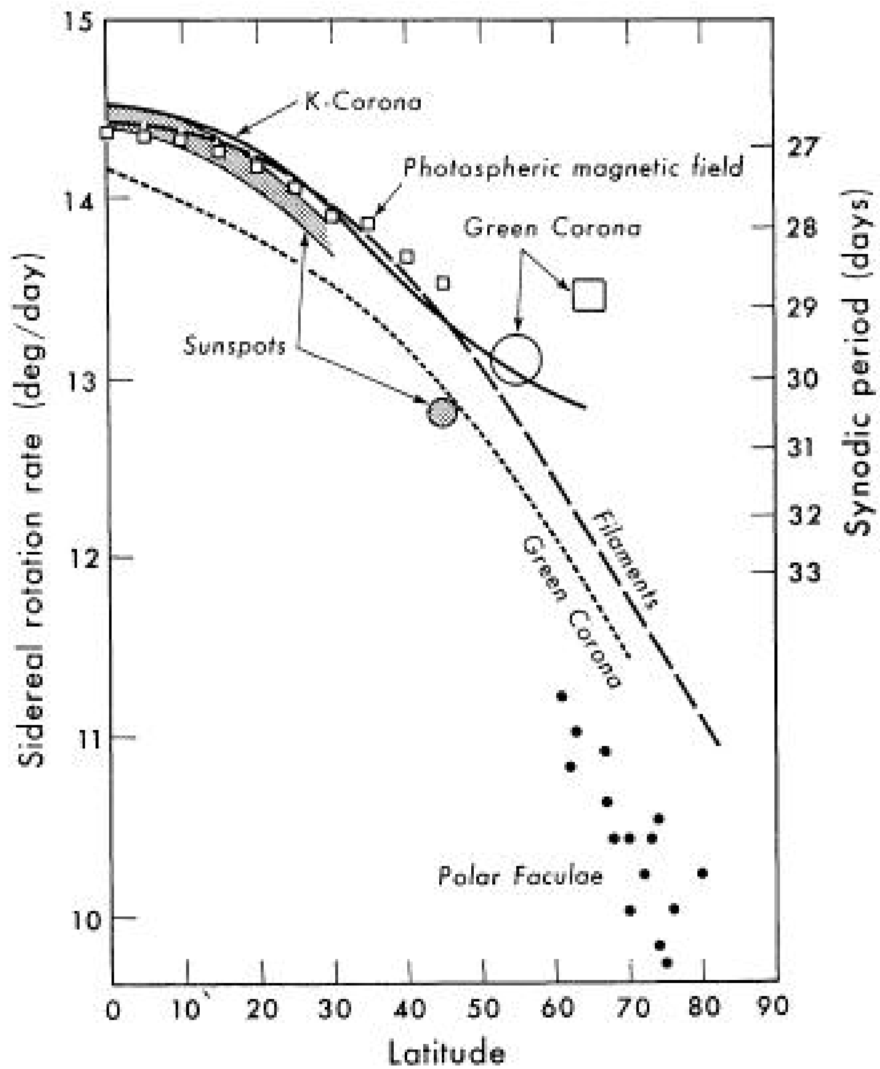

Typical proper motion pattern (deceleration) of sunspots interpreted by asymmetry of emerging flux loop]]

(van Driel-Gesztelyi & Petrovay, 1990; Caligari et al. 1995)

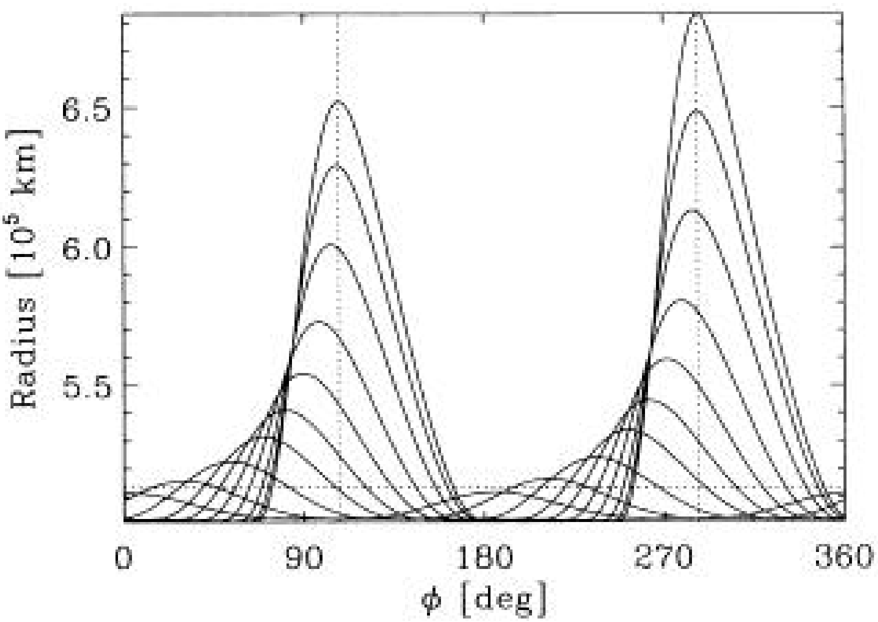

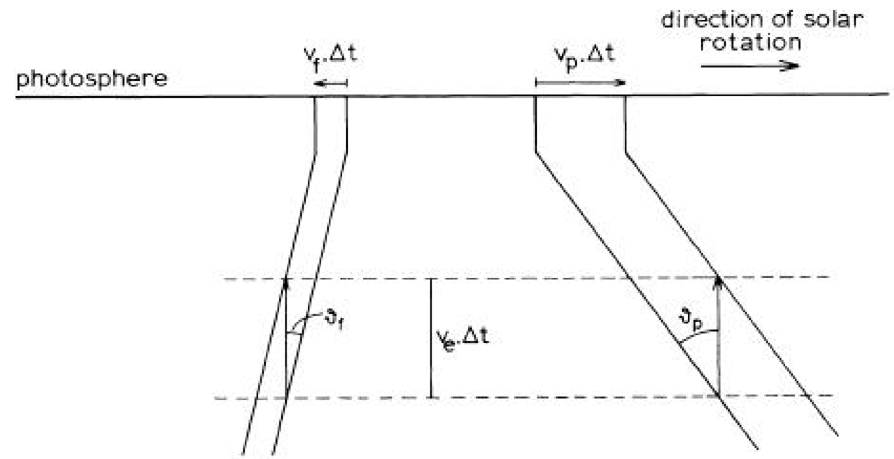

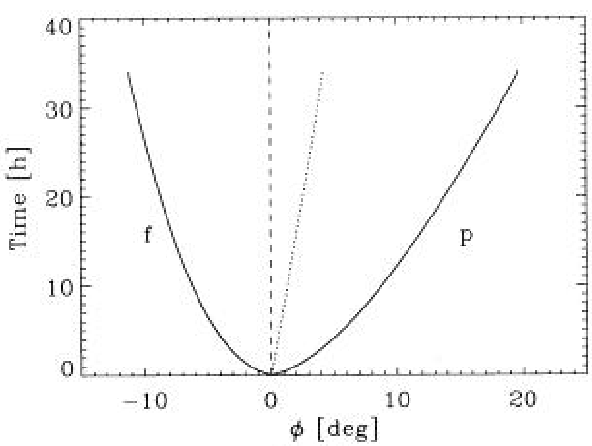

FIG. 14*a*

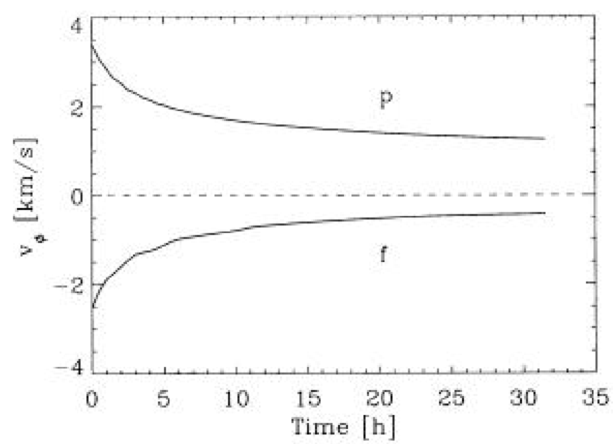

FIG. 14*b*

ROTATION OF LARGE-SCALE PATTERNS

Large-scale/long-time autocorrelations: found to be much closer to rigid rotation ($B \sim -0^{\circ}\!.4$/day). E.g.

– unipolar areas in photosphere (Wilcox et al. 1970);

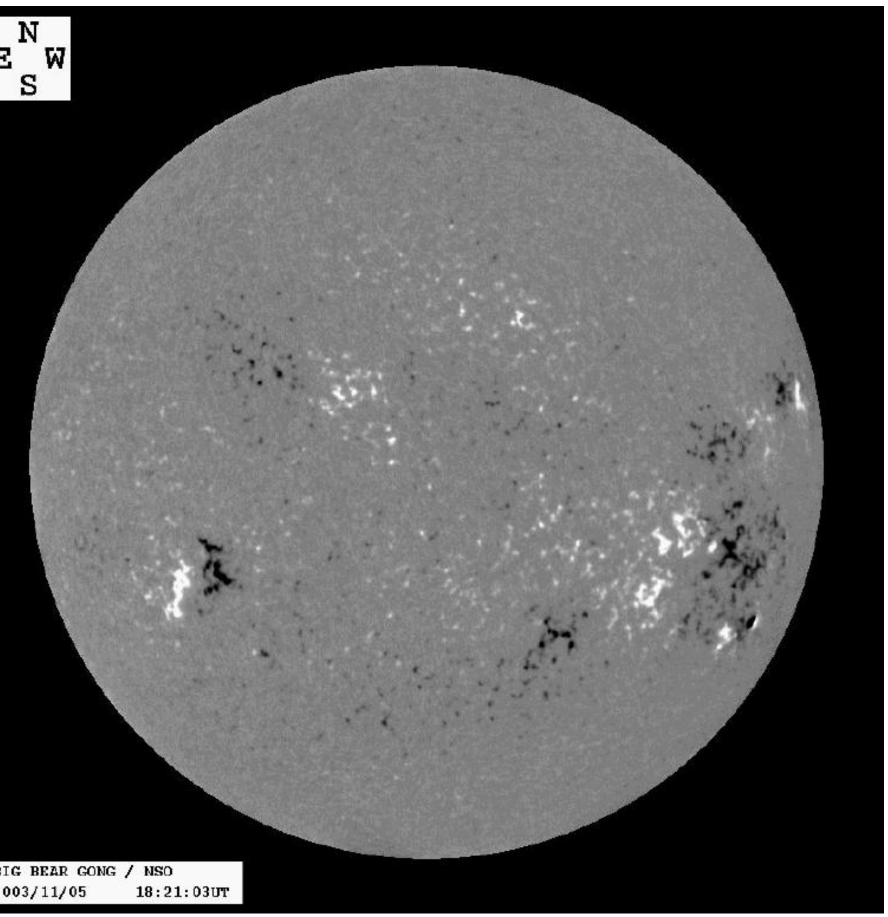

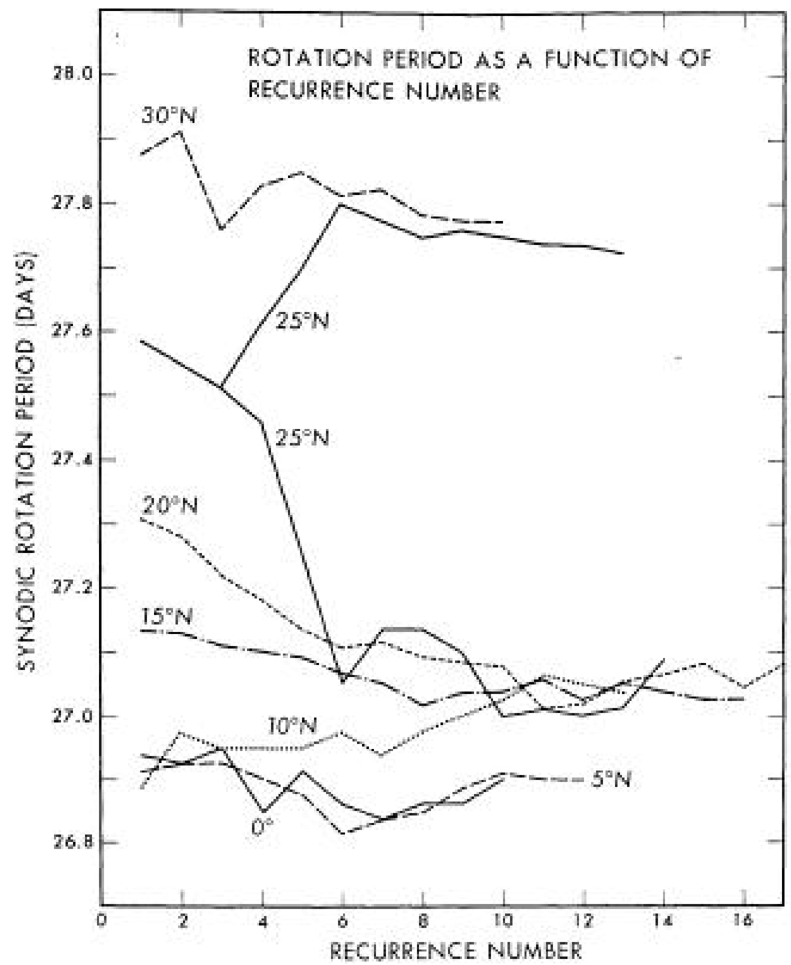

– coronal holes (Skylab's CH-1, 1973);

– interplanetary sector structure

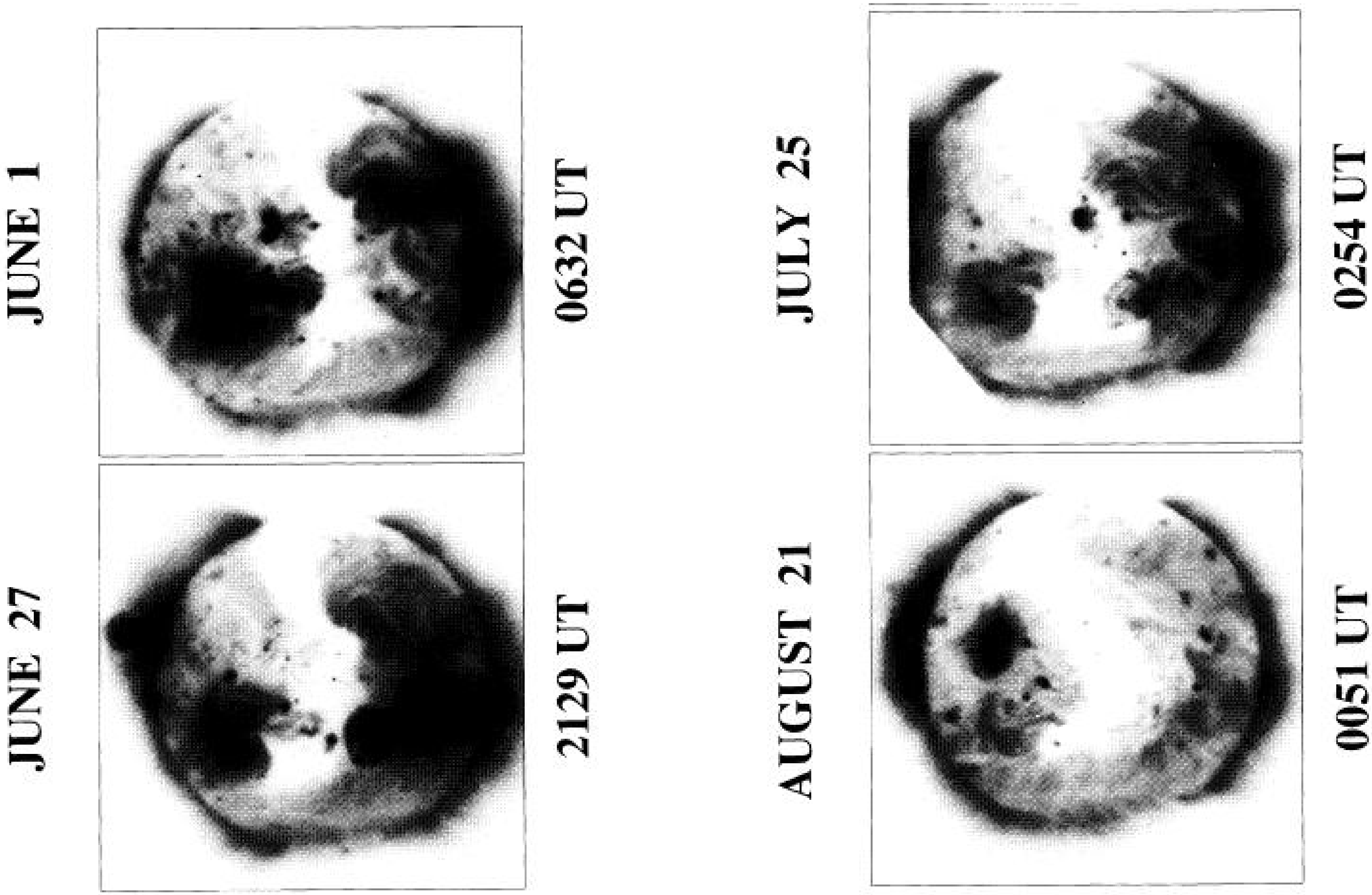

How can this be?

For unipolar areas

Stenflo (1988):
pattern of flux eruption from a subsurface layer.
But: rigid rot. much faster than rotation of radiative interior.

Sheeley et al. (1987):
Pattern rotation due to supergranular mixing of magnetic elements.

For coronal holes: "Reconnection wave" models

– Wang et al. (1988–93): Potential field model

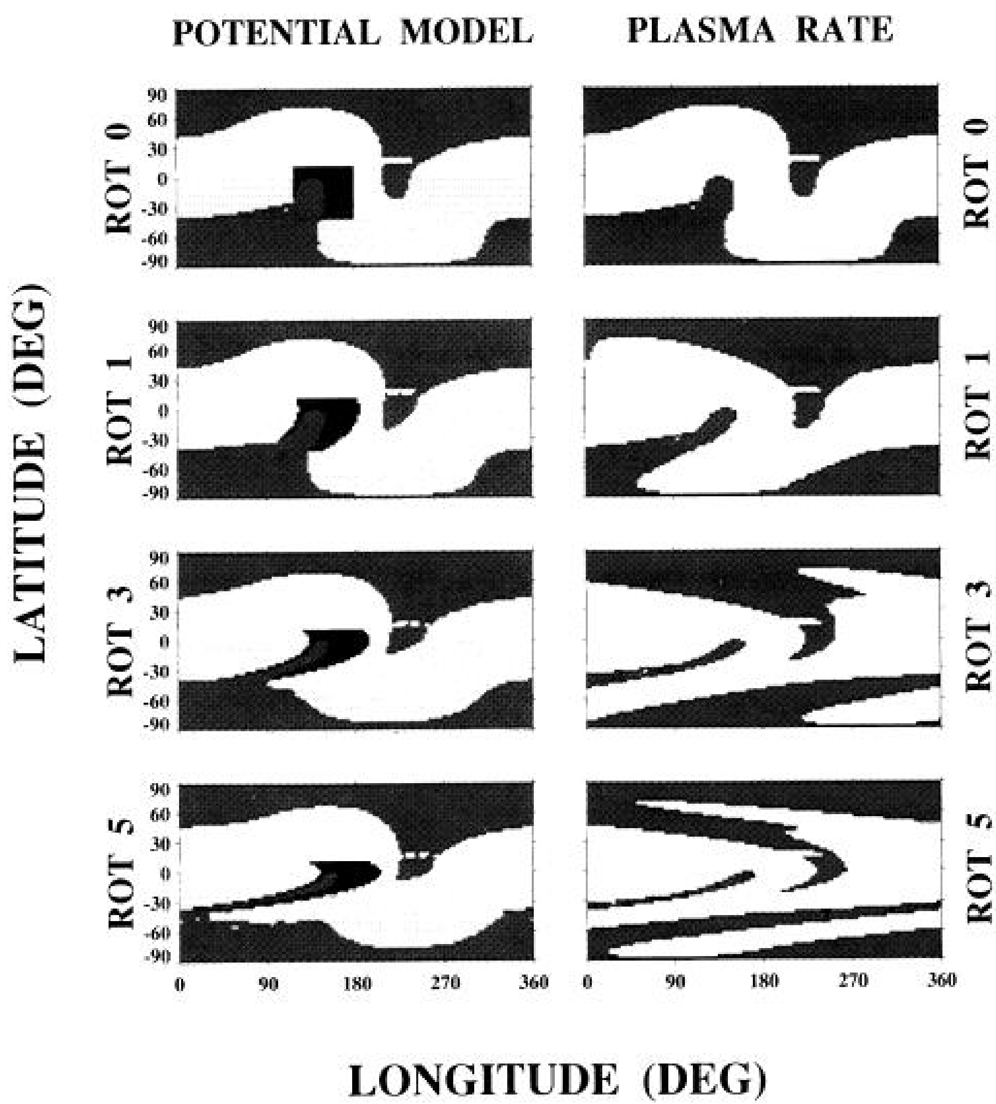

Assumption: coronal field is always nearly potential field, due to many small reconnection events.
(Some evidence from observations.)

Mechanism: Higher multipoles decline rapidly with height
⇒ rotation more rigid (e.g. for a tilted dipole, purely rigid).
Outer corona rotates rigidly ⇒ footpoint structures (=CHs) must also rotate rigidly, otherwise mg.field would wind up radially, and would not be current-free anymore
⇒ continuous reconnection must assure corotation.

Put in another way: Midlatitude holes form in external parts of unipolar area pairs. (If no other field on Sun, lines here would be open...) Polar CH extension forms by the polar CH connecting to a midhole CH.

CHs, i.e. footpoint pattern is determined by both axisym. comp. (=polar dipole) and nonaxisym component (AR) of phot.field.
But rotation of the pattern only depends on nonaxis.comp, irrespective of latitude
⇒ whole pattern rotates with the speed of the AR!

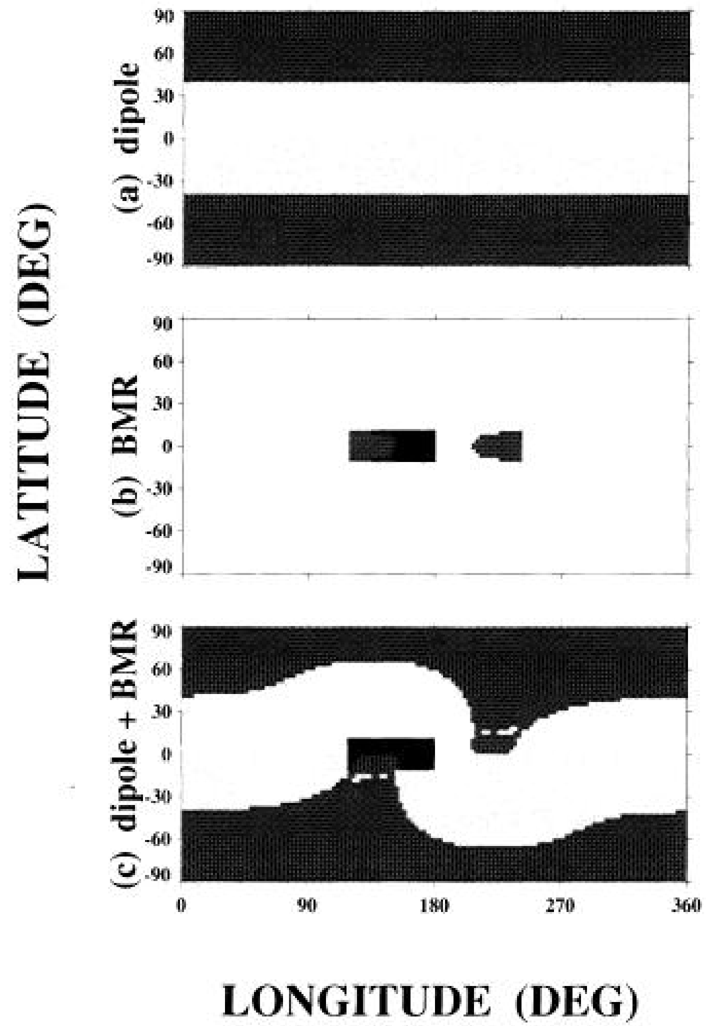

Cycle dependence:

Departures from rigid rotation caused by dif.rot. shear acting on AR/unipolar areas

⇒ amount of dif.rot. depends on size and latitude of ARs giving the nonaxis.component.

Very rigid if AR/unipolar flux concentrated and at low lat.

Less rigid if AR/unipolar flux spread and at high lat.

⇒ Rigid extensions most likely in declining phase of cycle; (∼Skylab)

Sheared extensions most likely in rising phase

Near max, no polar fields ⇒ small midlatitude holes, rotating differentially.

Seems to agree with observations.

BUT: alternative model proposed by Fisk et al.

Fisk et al. (1999): heliospheric binding model

Field cannot be potential at large distances, due to heliospheric current sheet.
Instead, at outer boundary (in heliosphere, at $r < r_A \sim 10 r_\odot$) magnetic pressure dominates:
$\nabla P_m = 0$ (i.e. field constant) + current sheet.

Tilted mg.axis (i.e. axis of polar CH) + diff.rot $\Rightarrow$ field lines rotate around the field line connecting to pole
$\Rightarrow$ field line footpoints (on outer surface) vary in latitude $\Rightarrow$ wind particles may change latitude (Fig.1)

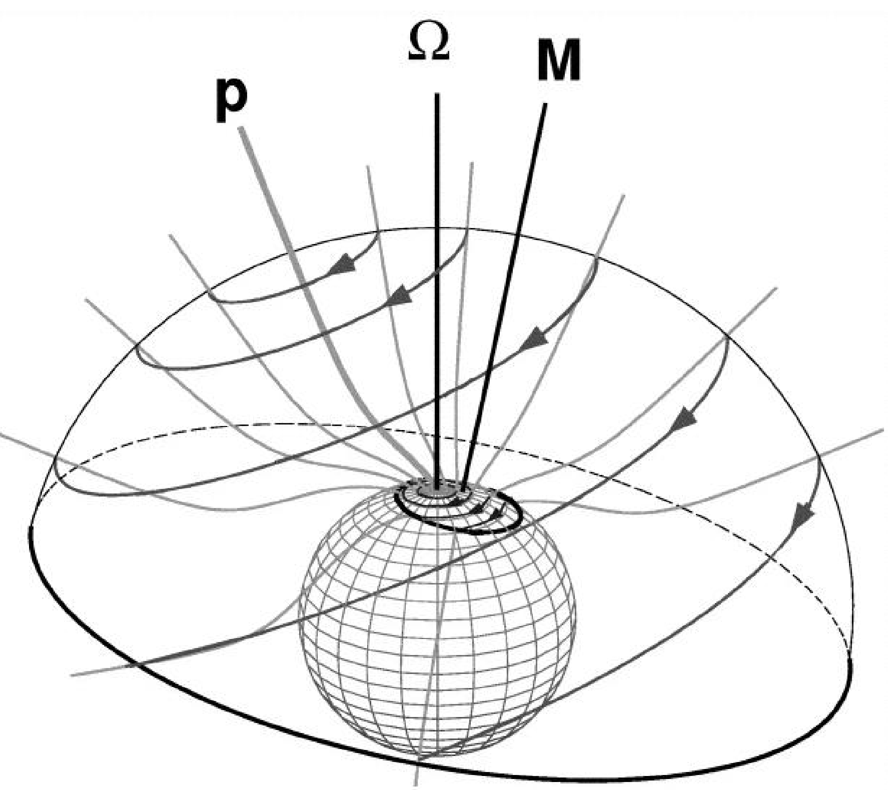

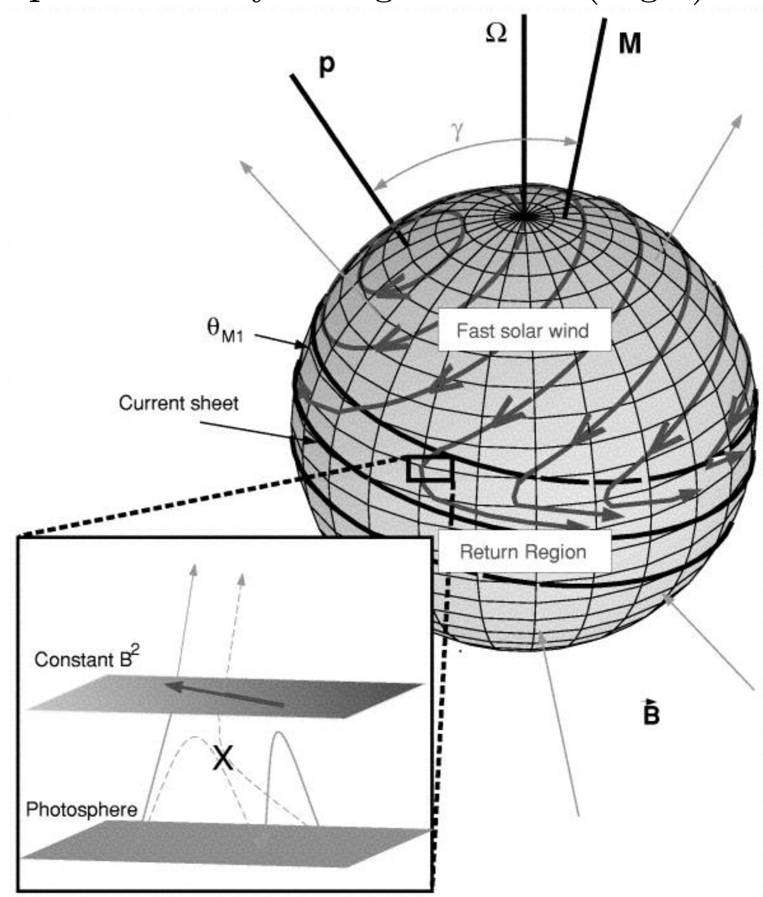

TORSIONAL OSCILLATIONS

Discovery: Howard & LaBonte (1980) in Doppler.

Detection by tracers: Snodgrass et al. (1985)

Seismic detection: Kosovichev & Schou (1997)

Poleward branch & depth dependence:
Ulrich (2001); Antia & Basu (2001); Howe et al. (2000)

Main mode: ~ 2/hemisphere.
Amplitude $\sim 0.1\,\%$ (a few nHz).

Phase locking with sunspot butterfly diagram:
$\partial\omega/\partial\theta$ in phase with activity.

They penetrate down to $\sim 70\,\mathrm{Mm}$, with downwards decreasing amplitude.

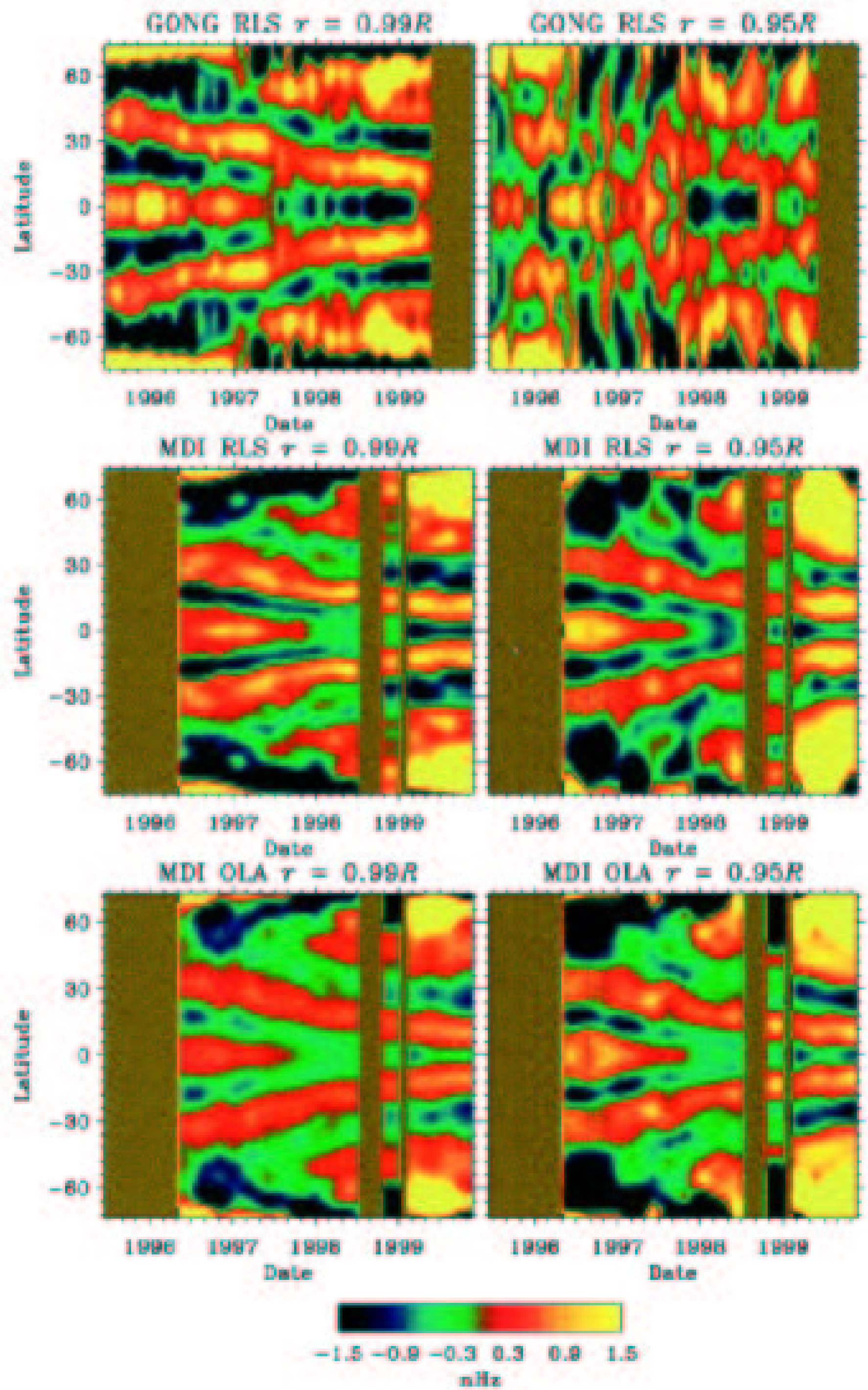

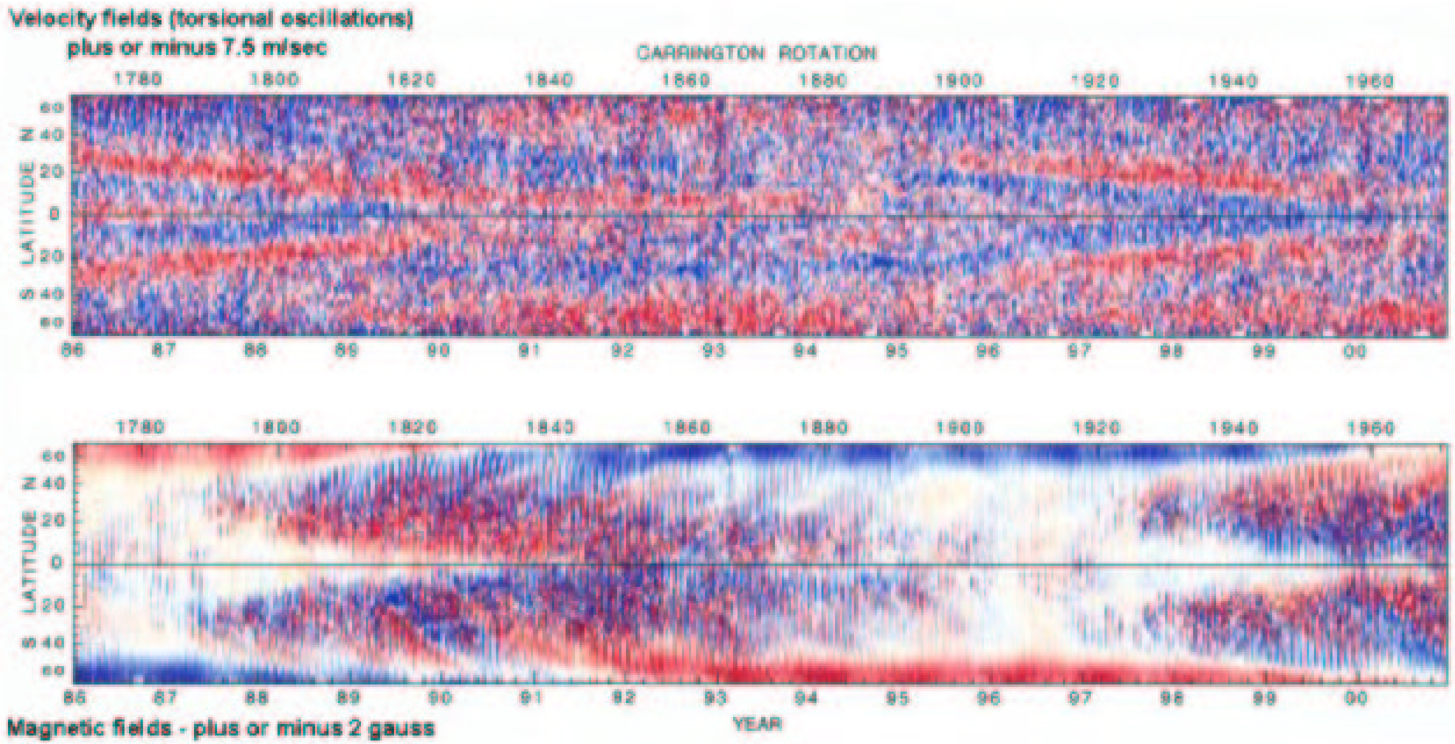

From Ulrich (2001) Red is faster than average velocity.

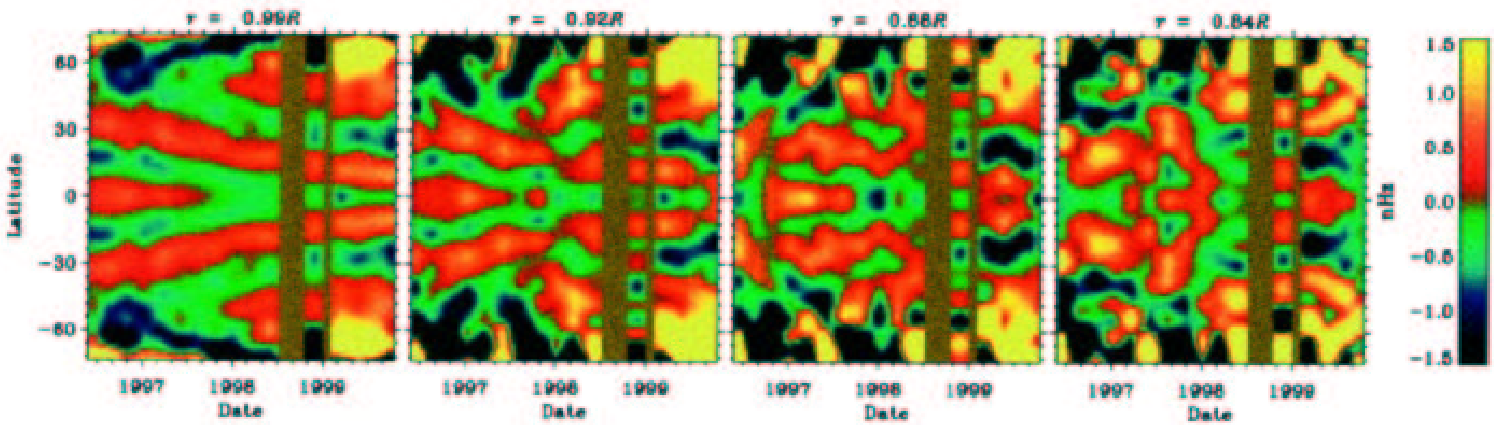

Phase locking with activity suggests magnetic origin.

Two main groups of theories:

Macrofeedback: T.O. driven by Lorentz force due to large-scale magnetic fields.

(Schüssler 1981, Yoshimura 1981, ..., Covas et al. 2001)

Microfeedback: T.O. due to magnetic modulation of turbulent driving of differential rotation.

(Küker et al. 1996, Kitchatinov et al. 1999, Petrovay & Forgács-Dajka 2001)

Microfeedback models:

+: observed depth-dependence

–: amplitudes tend to be too low

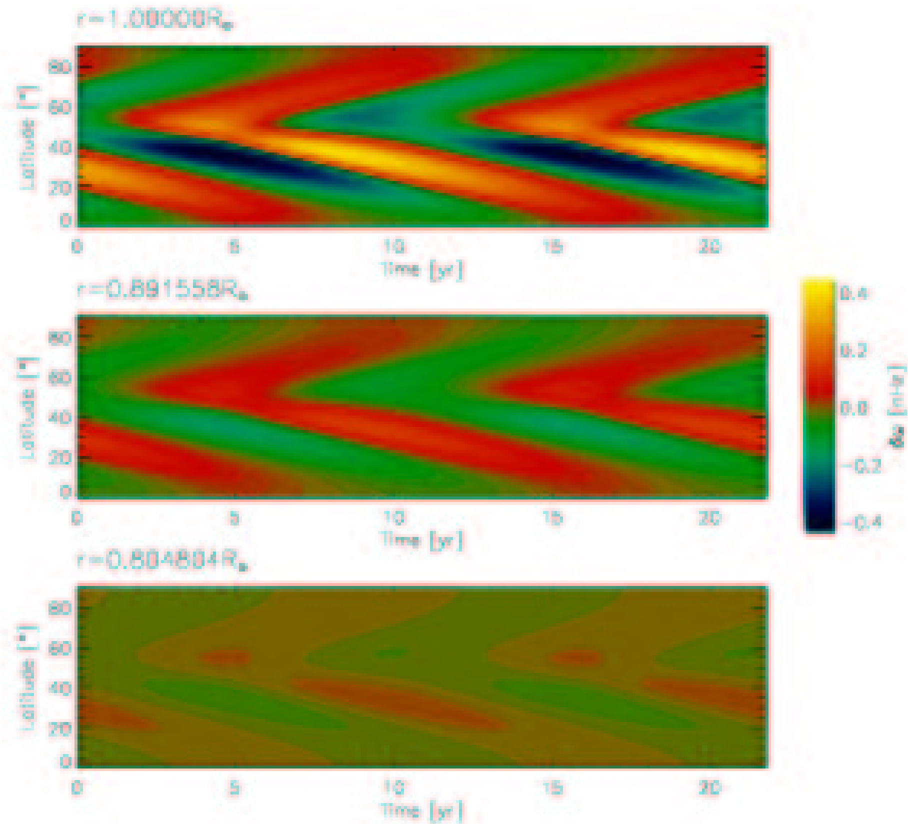

Petrovay & Forgács-Dajka (2001):

Extended plage fields ("crown" of the magnetic tree) suppress turbulent viscosity in shallow layers

⇒ increased shear in AR zone.

MERIDIONAL CIRCULATION

Doppler method:

Problem: measured lineshift is a brightness-weighted average.
Convective blueshift and limb shift (variation of blueshift with limb distance) $\gg$ merid.circ. signal. $\Rightarrow$ Doppler method not too good, contradictory results up to about 1987.

Main methods:

– compare E-W vs. N-S shifts.

– fit the signal with a superposition of dfferent effects

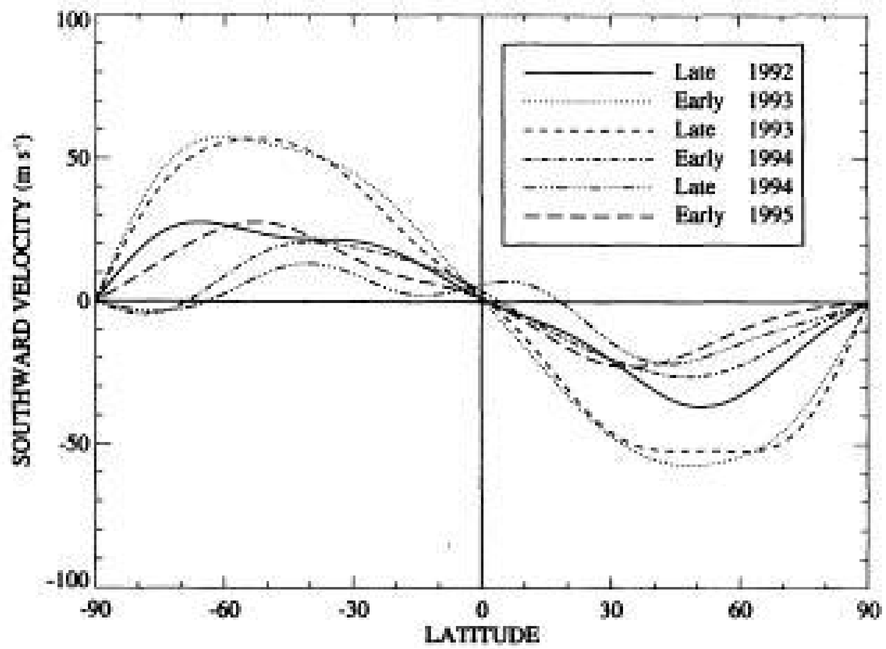

Mostly poleward flows reported from Duvall (1979) onwards, but strong latitude and/or time dependent fluctuations.

Clear poleward circ.: Ulrich et al (1988); then, esp. Cavallini et al. (1992)

Hathaway (1996): From GONG Doppler data. Poleward flow, strong variation on a timescale ∼months! (Speed occasionally up to 50 m/s!)

Tracer method:

Generally yields poleward flow of 10 m/s:

Topka et al. (1983) polar filaments;

Wang et al. magnetic patterns;

Komm et al. (1993), Latushko (1994),

Snodgrass & Dailey (1996): mg. cross-correlations

But: what do we measure exactly?

- Tracers may be independent of plasma

$\Rightarrow$ sunspots are basically useless.

- For smaller elements, may be just diffusion...

Can be sorted out by separating steady and cycle-related components.

General poleward flow, amplitude up to 13 m/s.

Superimposed on this, a migrating pattern of comparable amplitude, away from activity belts.

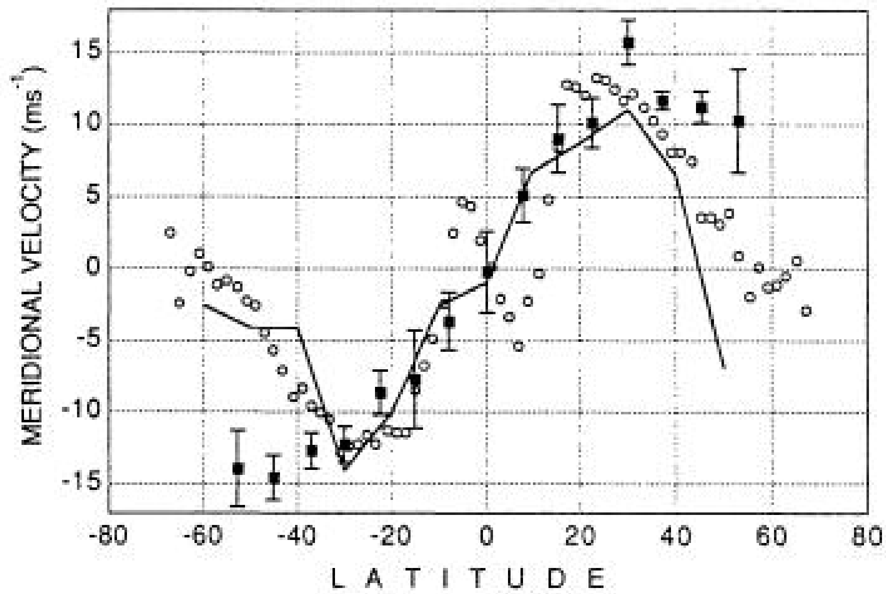

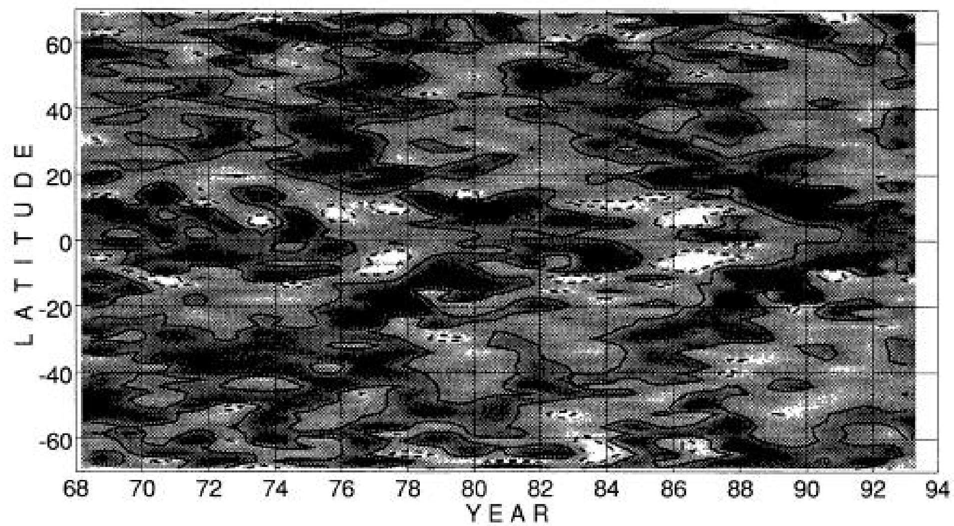

Seismic method:

Giles et al. (1997), Braun & Fan (1998),...,
Komm et al. (2004)

Poleward flow. Speed ∼10 m/s, seems to be maximal 4-5 Mm below surface.

Indication of northern polar countercell at depths of 7-12 Mm in MDI data. (Not present in GONG, maybe due to seeing effects.)